

RESEARCH ARTICLE

Copper transporter 1 (CTR1) expression by mouse testicular germ cells, but not Sertoli cells, is essential for functional spermatogenesis

Rashin Ghaffari¹, Kristin R. Di Bona², Christopher L. Riley¹, John H. Richburg^{1,2*}

1 Institute of Cellular and Molecular Biology, College of Natural Sciences, The University of Texas at Austin, Austin, TX, United States of America, **2** The Center for Molecular Carcinogenesis and Toxicology, Division of Pharmacology & Toxicology, College of Pharmacy, The University of Texas at Austin, Austin, TX, United States of America

* john.richburg@austin.utexas.edu



OPEN ACCESS

Citation: Ghaffari R, Di Bona KR, Riley CL, Richburg JH (2019) Copper transporter 1 (CTR1) expression by mouse testicular germ cells, but not Sertoli cells, is essential for functional spermatogenesis. PLoS ONE 14(4): e0215522. <https://doi.org/10.1371/journal.pone.0215522>

Editor: Suresh Yenugu, University of Hyderabad, INDIA

Received: August 13, 2018

Accepted: April 3, 2019

Published: April 19, 2019

Copyright: © 2019 Ghaffari et al. This is an open access article distributed under the terms of the [Creative Commons Attribution License](https://creativecommons.org/licenses/by/4.0/), which permits unrestricted use, distribution, and reproduction in any medium, provided the original author and source are credited.

Data Availability Statement: All relevant data are within the manuscript and its Supporting Information files.

Funding: This work was supported, in part, by the National Institutes of Health (2 R01ES016591; J.H.R.). Funding in the form of graduate research assistantship or teaching assistantship from The University of Texas at Austin was provided to R.G. and C.L.R. The funders had no role in study design, data collection and analysis, decision to publish, or

Abstract

An imbalance in copper (Cu) tissue homeostasis has a degenerative effect on spermatogenesis and male fertility. The high-affinity Cu transporter 1 (CTR1; SLC31A1) is the major protein responsible for Cu acquisition in eukaryotes and is highly expressed in mouse testes. Studies on yeast and *Drosophila* have demonstrated the conserved essential function of Cu and CTR1 for meiosis and fertility, implying that CTR1 may play an essential function in mammalian spermatogenesis. In mice, spermatogenesis takes place within the seminiferous epithelium, where tight junctions between somatic Sertoli cells (SCs) create a specialized microenvironment for the development of meiotic germ cells (GCs) by tightly regulating the free transport of metabolites and ions to reach these cells. Here, it is demonstrated that within the seminiferous epithelium, CTR1 is expressed on the membrane of primary pachytene spermatocytes and SCs. To examine the physiological significance of CTR1 in spermatogenesis, mice with a GC-specific (*Ctr1^{ΔGC}*) and SC-specific (*Ctr1^{ΔSC}*) disruption of the *Ctr1* gene were generated. The testis of *Ctr1^{ΔGC}* mice exhibits a severe progressive loss of GCs starting at postnatal day (PND) 28 leading to testis hypoplasia by adulthood. No spermatogenic recovery was observed in *Ctr1^{ΔGC}* testis beyond PND 41, despite the presence of FOXO-1 expressing undifferentiated spermatogonial cells. However, *Ctr1^{ΔSC}* mice displayed functional spermatogenesis and were fertile, even though testicular Cu levels and Cu-dependent cellular activities were significantly reduced. These results reveal, for the first time, the importance of CTR1 expression by GCs for maintaining functional spermatogenesis.

Introduction

Copper (Cu) is an essential trace metal that is required for all organisms due to its important roles in growth and development. Cu serves as an important co-factor for enzymes that

preparation of the manuscript. No commercial funding supported this work.

Competing interests: The authors have declared that no competing interests exist.

carryout fundamental biological processes including respiration (cytochrome c oxidase), elimination of free radicals (superoxide dismutase), iron metabolism (ceruloplasmin), connective tissue formation (lysyl oxidase) and many others [1,2]. On the other hand, excess Cu can create a toxic environment in the host cell by producing reactive oxygen species [3,4]. Consequently, alterations of Cu levels and the activities of Cu-dependent enzymes lead to disease and pathophysiological conditions including Wilson's and Menke's disease, and ataxia [1,3]. The importance of Cu in spermatogenesis has been documented in various animal studies [5]. Induced Cu deficiencies in male rats, goat and rams result in reduced sperm counts and motility, poor semen quality and an abnormal germinal epithelium [6–8]. These effects were reversible upon Cu supplementation indicating the importance of Cu in the maintenance of male fertility and spermatogenesis [6–8].

Spermatogenesis is a complex process in which spermatogonial stem cells (SSCs) proliferate and their progeny (spermatogonia) undergo many successive mitotic divisions ending with the development of meiotic cells (spermatocytes). Spermatocytes subsequently undergo two meiotic divisions leading to the production of haploid cells (spermatids) that further differentiate to give rise to spermatozoa. This process takes place in the seminiferous epithelium of the mammalian testis and is largely orchestrated by the somatic Sertoli cells (SCs) [9]. Specialized tight junctions between adjacent SCs creates a barrier known as blood-testis barrier (BTB) that creates two compartments: a basal compartment below the BTB and adluminal above. The basal compartment is where mitotic spermatogonial cells reside and the adluminal compartment is where meiotic spermatocytes, spermatids and spermatozoa are found. The BTB regulates the free transport of metabolites, ions or harmful substances from entering lumen of the seminiferous tubules and reaching the meiotic germ cells (GCs) [10]. Many different transporters are expressed in testis, either by the SCs or GCs, to facilitate the influx and/or efflux of metabolites and create a suitable environment for spermatogenesis to take place [11].

Organisms regulate Cu homeostasis via various proteins responsible for regulating Cu transport, intracellular trafficking and storage [2,12]. The Cu transporter 1 (SLC31A1; *CTR1*) is a high affinity Cu transporter, conserved from yeast to humans, which functions as a major Cu importer across the plasma membrane [13,14]. The loss of *Ctr1* is embryonically lethal in mice, further confirming its essential function in developmental physiology [15]. The *Ctr1* gene is broadly expressed in all tissues of the mouse however, the relative tissue distribution varies with liver, kidney, and testis expressing higher mRNA levels, while brain and muscle express lower levels [15–18].

There is a growing body of evidence on the effects of Cu and *Ctr1* expression on meiosis and male fertility in eukaryotes. In the *Schizosaccharomyces pombe* *Ctr4*, the yeast homolog of mammalian *Ctr1*, is highly expressed on the cell surface during early meiosis by which cells undergo meiotic arrest at metaphase I in a Cu deficient environment [19,20]. Furthermore, in *Drosophila* the *CTR1*-like protein, *Ctr1C*, also shown to be associated with male fertility [21]. In *Drosophila* endogenous *Ctr1C* is expressed in mature spermatocytes and spermatozoa while an alternate transcript, *Ctr1B* is expressed in the intestine. Lack of *Ctr1C* in mutant background lacking intestinal *Ctr1B*, lead to male sterility in *Drosophila* [21]. A recent report evaluating the expression profile of Cu regulatory proteins in the mouse testis indicated that the *CTR1* protein is mainly observed in the adluminal compartment of the seminiferous epithelium where primary spermatocytes reside [22]. Together, these observations strongly implicate *Ctr1* as an important factor for mammalian spermatogenesis. In this study the physiological significance of *Ctr1* in both GCs and in SCs is independently characterized for its importance in functional spermatogenesis.

Materials and methods

Generation of germ cell- and Sertoli cell- specific *Ctrl* knockout mice

The GC and SC specific *Ctrl* knockout mice were generated using the *Cre-loxp* system. The transgenic mice strains *Ddx4-Cre* (GC-specific Cre strain number 006954, also known as *Vasa-Cre* [23]) and *Amh-Cre* (SC-specific Cre Stock number 007915 [24]) were purchased from The Jackson Laboratory (Bar Harbor, ME). The *Ctrl*^{fl/+} mice were generously provided by Dr. Dennis Thiele (Duke University, NC [25]) and maintained in breeding colonies throughout experiments. Mice colonies were kept in a controlled temperature (23°C ± 1°C) and light (12 L:12 D) environment. Standard chow (5LL2, Purina Mills Lab-Diet, St. Louis, MO) and tap water were supplied *ad libitum*. All procedures were performed in accordance with established guidelines and approval from The University of Texas at Austin's Institutional Animal Care and Use Committee (Protocol ID: AUP-2015-00198).

Initially, homozygous *Ctrl*^{fl/fl} female mice were crossed with male mice carrying either *Ddx4*- or *Amh-Cre* gene, which expresses *Cre* recombinase under the control of *Ddx4* or *Amh* gene promoter, respectively. *Ddx4* expression is activated in early GCs (gonocytes or prospermatogonia) on embryonic (E) days 15–18, and *Amh-Cre* is activated as early as E14.5 in SCs [23,24]. The heterozygous mice carrying either *Ddx4-Cre; Ctrl*^{+/fl} or *Amh-Cre; Ctrl*^{+/fl} genotype from the initial cross were then back-crossed to *Ctrl*^{fl/fl} female mice to obtain GC (*Ctrl*^{ΔGC}) or SC specific (*Ctrl*^{ΔSC}) *Ctrl* knockouts (S1A Fig). Wild-type littermates carrying *Ctrl*^{fl/fl} gene with no *Cre* gene expression were used as control mice (WT). Genotypic conformation was performed via PCR of genomic DNA with the AccuStart II Mouse Genotyping Kit (95135–500, Quanta BioSciences, Gaithersburg, MD, USA,) using primers specific for the presence of the *Amh-Cre* transgene: 5' – TGG TTT CCC GCA GAA CCT GAA G–3' (forward); 5' – GAG CCT GTT TTG CAG GTT CAC C–3' (reverse), *Ddx4-Cre* transgene: 5' –CAG GGT GTT ATA AGC AAT CCC–3' (forward); 5' –CCT GGA AAA TGC TTC TGT CCG–3' (reverse) and the *Ctrl*-LoxP gene: 5' –AATGTCTGGTGCCTGCTGAAA–3' (LoxA838U); 5' –GCAGTAGATAAAAAGCCAAGGC–3' (LoxA1052L) [25] (S1B Fig)

Tissue collection

Mice at postnatal day (PND) ages 14, 28, 41, 60, 70 were either euthanized by CO₂ asphyxiation followed by cervical dislocation for histological, protein and RNA assay and for metal measurements purposes. Both testes were rapidly removed, weighed, and either flash frozen in liquid nitrogen and stored at -80°C or immersed in Bouin's solution (R1121000, RICCA Chemical Company, Arlington, TX).

Histology and immunohistochemistry

Testes were collected and fixed in Bouin's solution overnight at room temperature, then washed in lithium saturated 70% ethanol and embedded in paraffin. Paraffin-embedded testis was sectioned to a thickness of 5 μm. Sections were then deparaffinized and rehydrated in a graded series of ethanol solution in order to perform histology and immunohistochemical detection of the primary antibodies.

For morphological analyses, testis sections were stained with periodic acid-Schiff-hematoxylin (PAS-H) and mounted on glass slides according to standard protocols [26].

Immunohistological staining was performed according to established protocols [27] using VectaStain ABC kit (PK6101, Vector Laboratories, Burlington, CA, USA) and 3–3'-diaminobenzidine (DAB) substrate (SK-4100, Vector Laboratories). Testis cross sections were first incubated in 10% normal horse serum blocking buffer (Sigma-Aldrich, St. Louis, MO) for an

hour at room temperature. Cross sections were then incubated overnight at 4°C with the specific primary antibody diluted in 10% horse serum blocking buffer, including rabbit polyclonal anti-CTR1 (1:500, 071314/1-2; kindly provided by Dr. Dennis Thiele [25]), and rabbit anti-FOXO-1 (1:100, 2880, Cell Signaling Technologies Inc. Danvers, MA), or incubated for one hour at room temperature with either rabbit anti-PCNA (1:200, ab18197, Abcam, Cambridge, MA), or polyclonal rabbit anti-SOX9 (1:200, AB5535, EMD Millipore, Burlington, MA).

Histological sections were imaged using a Nikon Eclipse microscope and captured using Nikon digital sight DS-Fi1 camera. Images were analyzed using NIS Elements (version 3.2 64 Bit) and ImageJ (version 1.50i) software.

Assessment of Sertoli cell numbers

The SC marker, SOX9, was used to determine the average number of SCs per tubule for each genotype [27]. The average number of SCs per tubule was calculated by counting SOX9 positively nuclear stained cells in each round seminiferous tubule (> 100 tubules per mouse per genotype). A total of 3 animals per genotype were analyzed.

TUNEL assay for apoptosis

Terminal deoxynucleotidyl transferase dUTP nick end labeling (TUNEL) staining was used to assess GC apoptosis in paraffin-embedded testis cross sections. TUNEL assay was performed using the ApopTag Peroxidase *In Situ* Apoptosis Detection Kit (S7100, EMD Millipore). The apoptotic index (AI) was calculated as the percentage of essentially round seminiferous tubules cross sections containing > 3 TUNEL-positive GCs [28]. More than 100 seminiferous tubules per cross section were quantified per animal. A total of 3 animals per genotype per age group were analyzed.

Sertoli cell isolation

The SC isolation procedure was performed as described previously Karzai et al. with minor modifications [29]. Testes of PND 25 mice were collected, detunicated and processed through two rounds of enzymatic digestions (0.1% collagenase, 0.2% hyaluronidase, 0.03% DNaseI, 0.03% Soybean trypsin inhibitor, pH7.4) at 34°C, 80 oscillations/min for 25 minutes each. Cells were then washed with Hanks solution twice, followed by two rounds of enzymatic digestions (0.1% collagenase–dispase, 0.2% hyaluronidase, 0.03% DNaseI, 0.03% Soybean trypsin inhibitor, pH7.4). Cells were washed twice with Hanks solution and then filtered through a 70–100 µm Nitex membrane and the flow through cells were collected and plated. Cells were plated (3–4 × 10⁶ cells per 60mm plate) in laminin coated 60 mm plates and incubated at 35°C (95% O₂ and 5% CO₂). Media was changed every 24 hours to remove unattached GC contaminants. By day 7, SCs cells were either collected for RNA or protein assays. The purity of the SC culture was assessed using *in situ* staining of SOX9 antibody. The procedure yielded approximately 85–90% SC purity.

Quantitative-PCR

RNA from primary SC cultures was collected using PureLink RNA Mini Kit (12183020, Ambion) according to the manufactures protocol. A total of 500 ng RNA was used to make cDNA. Q-PCR was performed on each cDNA sample of 10 µl volume containing 1 µl of 20 ng cDNA, 1x of iTaq Universal SYBR Green Supermix (1725120, Bio-Rad Laboratories Inc., Hercules, CA) and 250 nM forward and reverse primers for *Ctr1*: 5′ –GGGGCTTACCCTGTGAAGACTTT–3′ (forward); 5′ –CGTCCGTGTGGTTCATACCC–3′ (reverse). Relative mRNA expression for the gene of interest was normalized against the housekeeping gene Hypoxanthine guanine phosphoribosyl transferase 1 (*hprt1*) [30]: 5′ –CAGTCCCAGCTCGTGATTA–3′

(forward); 5' -TGGCCTCCCATCTCCTTCAT -3' (reverse) using the $\Delta\Delta$ CT method as described in Applied Biosystems User Bulletin No. 2 (P/N 4303859).

Membrane preparation for CTR1 protein detection

Crude membrane preparations from primary SC pellets were homogenized with homogenizing buffer containing 10 mM Tris-HCL, 1 mM EDTA, 250mM NaCl and Mini Protease Inhibitor (88666, Thermo Scientific, Waltham, MA) and incubated at 4°C for 10 minutes. The cell homogenates were centrifuged at 21,000 g at 4°C for 15 minutes. The supernatant (cytosolic fraction) was removed, and the pellet was re-suspended in homogenizing buffer containing 1% Triton X-100. The solution was then incubated at 4°C for 30 minutes and centrifuged with 21,000 g 4°C for 5 minutes. The supernatant was collected as crude membrane fraction and used for immunoblotting against CTR1 antibody (as described below).

Immunoblotting

Protein lysates were prepared from mice testis by homogenizing in RIPA buffer containing 1% Triton X-100, 1 mM EDTA, 0.1% SDS; freshly prepared with complete Mini Protease Inhibitor (88666, Thermo Scientific). Protein concentrations were measured using bicinchoninic acid (BCA) assay (23224, 23228, Thermo Scientific) with bovine serum albumin (23210, Thermo Scientific) as standard. A total of 20 μ g of protein lysates were ran through SDS-PAGE gel and transferred onto Polyvinylidene Fluoride (PVDF) membrane. The PVDF membrane was first blocked with 5% milk and probed overnight at 4°C with either mouse monoclonal anti-CCS (1:100, sc-374205, Santa Cruz, Dallas, TX), or rabbit polyclonal anti-SOD1 (1:100, NBP2-24915, Novus, Littleton, CO), or rabbit polyclonal anti-COX5A (1:500, C1129A, CusAb), or rabbit anti-GAPDH (1:1000, 5174S, Cell Signaling) all diluted in 2.5% milk.

Western blotting for CTR1 was performed on membrane enriched primary SCs (20 μ g) lysates. A rabbit polyclonal anti-CTR1 was generated and affinity purified of the antigen peptide H_2N - VSIRYNSMPVPGPNGTILC-CO₂H, which corresponds to the cytosolic loop between transmembrane domains 1 and 2 of mouse and human CTR1 by Bethyl laboratories (Montgomery, TX). The CTR1 antibody (1:1000 dilution) was incubated overnight at 4°C in 2.5% milk. Overnight incubation at 4°C with rabbit polyclonal anti-Sodium/Potassium pump (1:100, SC-28800, Santa Cruz) was used as a plasma membrane protein marker.

Either HRP-conjugated mouse-IgG (1:1000 dilution) or rabbit-IgG (1:2500 dilution) was used as the appropriate secondary antibody for immunoblotting. The protein bands were visualized using ECL reagent (GE healthcare RPN2232) as described by the manufacturer.

Cytochrome c oxidase activity assay

Cytochrome c oxidase (CCO) activity assay was performed according established protocols [31]. A total of 10 μ g of protein lysates from adult testis and 15 μ g primary SCs protein lysates of both *Ctr1*^{ASC} and WT were used. A solution of 100 mM potassium phosphate buffer (pH 7.0) and 1 mM of reduced cytochrome c was first measured for baseline activity at 550 nm for 2 minutes. The enzyme activity was calculated from the decrease rate of absorbance of cytochrome c at 550 nm ($\xi = 18.5 \text{ nM}^{-1} \text{ cm}^{-1}$) for 3 minutes following the addition of the samples. Since the estimate of the CCO enzyme activity depends on the amount of mitochondria within the tissue or cell, the CCO activity was normalized to the activity of citrate synthase enzyme, a mitochondrial matrix enzyme used as marker of the abundance of mitochondria. Citrate synthase was assayed by the reduction of 1 mM of 5,5'-Dithiobis (2-nitrobenzoic acid) (DTNB) in the sample containing 200 mM Tris buffer (pH 8.0) with Triton X-100 (0.2% (vol/vol)), 10 mM of acetyl CoA, and 10 mM oxaloacetic acid. The increase in absorbance was

monitored at 412 nm for 3 minutes ($\xi = 13.6 \text{ mM}^{-1} \text{ cm}^{-1}$). Cells and tissues samples of three animals from each genotype were used for analysis.

Testicular spermatid head counts

To estimate sperm production from each genotype, testicular spermatid head counts were performed as previously described with a few modifications [32]. Testis from each mouse was homogenized in 10% DMSO/Saline solution. Cell suspension was then centrifuged at 7,500 rpm for 2 minutes. The pellet was re-suspended in DMSO/Saline solution and was diluted 1:1 ratio in 0.1% Trypan-blue stain (15250–016, GIBCO, ThermoFisher,). The sperm suspension was loaded onto a hemocytometer and the number of spermatid heads was counted via light microscopy. Three animals from each genotype were analyzed.

Total metal measurements

Testes and seminiferous tubules were collected and weighed into acid washed vials (175–54, Savillex) and dried overnight at 85°C. Dried tissues were then digested overnight into 1 ml of trace-analysis grade nitric acid (225711, Sigma) at 85°C. Metal measurements of the primary SCs were performed according to Zogzas et. al. with few modifications [33]. On day 7 of primary SC culture, cells were washed with cold phosphate buffered saline (PBS) and harvested by trypsin and pelleted. Cell pellets were then washed twice with PBS supplemented with 10 mM EDTA. Before the final wash, pellet was re-suspended in EDTA-free PBS and the number of cells were counted using Trypan-blue (T8154, Sigma) using hemocytometer for each pellet per animal. Following the final wash, PBS supernatant were aspirated completely, and pellets were directly digested in 200 μl of trace-analysis grade nitric acid and incubated at 85°C overnight. Both tissue and primary cell samples were brought to room temperature and reduced nitric acid concentration to 2% nitric acid with ultra-pure water (10977–015, life Technologies). Samples were then sent to inductively coupled plasma- mass spectrometry (ICP-MS) core facility in Jackson School of Geosciences, of the University of Texas at Austin for analysis.

Statistical analyses

Statistical analyses were performed utilizing GraphPad Prism version 7.03 for Windows. Data are presented as the means \pm SD and analyzed using unpaired t-tests corrected for multiple comparisons using the Holm-Sidak method. Statistical significance was considered when $p < 0.05$ unless otherwise stated.

Results

CTR1 is expressed in pachytene spermatocytes and in Sertoli cells in a stage specific manner

To ascertain the specific cellular localization of CTR1 protein within seminiferous epithelium, immunohistochemical analysis was performed with a previously well-characterized specific antibody of CTR1 that was examined across mammalian species [34]. The localization of CTR1 protein in testicular cross sections of PND 60 wild-type (WT, *Ctr1*^{fl/fl}) mice testes indicated that within the seminiferous tubules, CTR1 localized to the plasma membrane of primary spermatocytes and along both the basal and adluminal compartments of SCs (Fig 1A and 1B). The specificity of the CTR1 antibody was confirmed on adult intestine cross sections (Fig 1D), which show CTR1 expression on the apical membrane of the intestinal epithelial cells, consistent with previous reports [25,34]. Secondary only negative control is shown in Fig 1C and 1E.

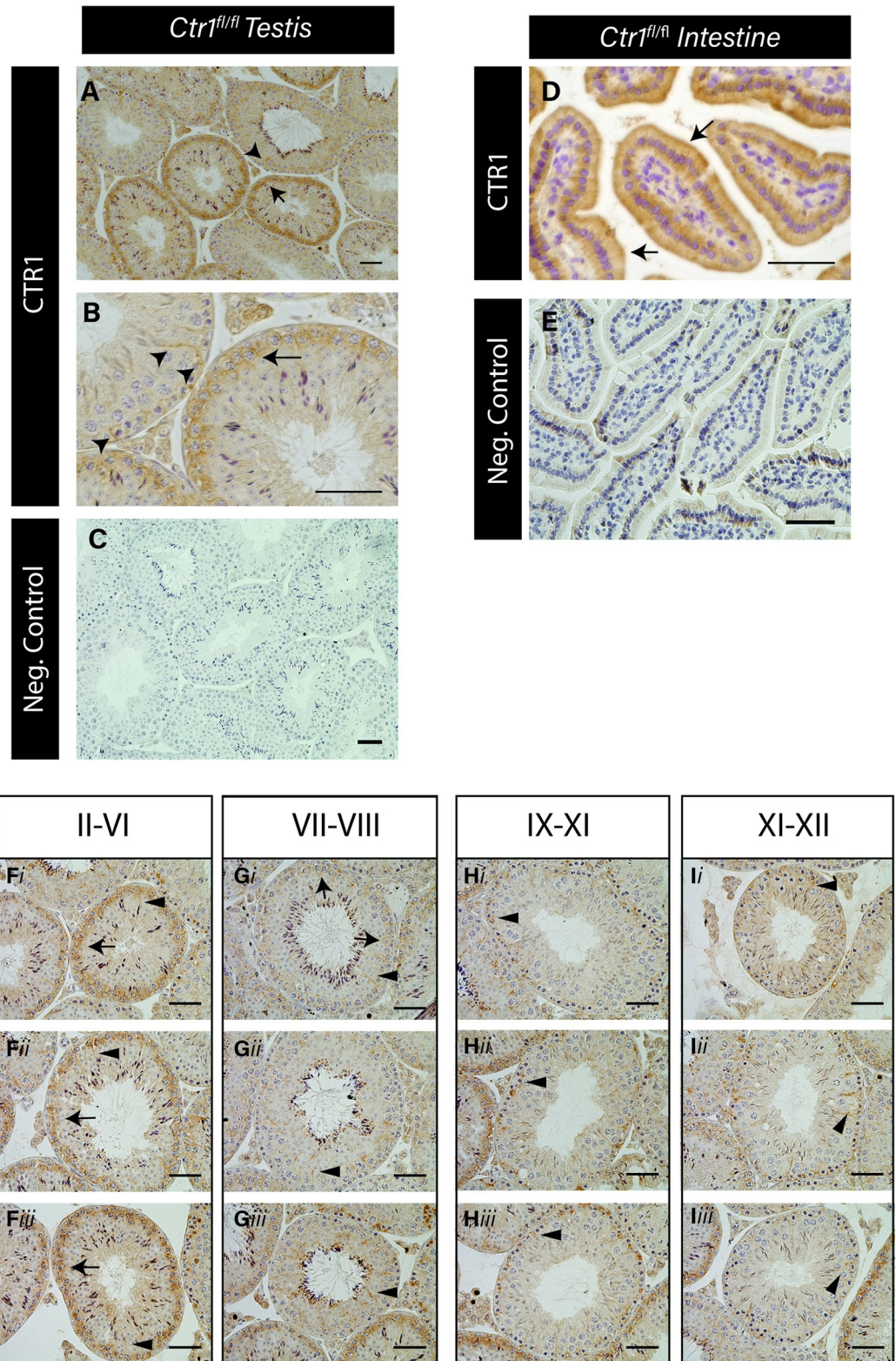


Fig 1. CTR1 is expressed in pachytene spermatocytes and Sertoli cells in a stage specific manner. Immunohistochemical localization of CTR1 in adult (PND 60) *Ctrl^{fl/fl}* mouse testis cross sections (A, B). Arrow indicates expression on primary pachytene spermatocytes. Arrowheads indicate SC apical and basal cytoplasm. CTR1 expression on the apical surface of the epithelial cell in the intestine of adult mice indicated by arrows (D). Negative secondary only control of testis (C) and

intestine (E) shown. Scale bar = 50 μm . Seminiferous epithelium at stages II-VI displayed the highest *CTR1* expression on pachytene spermatocytes (F). Stages VII-XII (G, H and I) display the least *CTR1* staining on primary spermatocytes (arrows) but high *CTR1* localization on SCs (indicated by arrowheads) within the seminiferous tubule cross sections. Three different tubule cross sections for each specified stage are shown below each grouped of stages (i-iii). Scale bar = 100 μm .

<https://doi.org/10.1371/journal.pone.0215522.g001>

Immunohistochemical analysis on testis cross sections revealed a stage specific pattern of *CTR1* protein expression within the seminiferous tubules. In histological cross section of mammalian testis, recurring of multiple GCs at various stages of development are always found associated together within a linear segment of seminiferous tubules. These recurring GC associations goes through defined cycles within seminiferous tubules that are referred to as stages, ranging from I to XII, of spermatogenic cycle in mice (for review, see [9,35]). Histological stages of the seminiferous epithelium in WT mouse testis cross sections were estimated by assessing the shape of spermatid heads, acrosomal cap, presence and location of preleptotene spermatocytes [35]. The stages were accordingly grouped as II-VI, VII-VIII, IX-XI and XII. Fig 1F illustrates that *CTR1* expression detected on primary pachytene spermatocytes was highest in tubules at stages II to VI, and in few tubules at stages VII-VIII (Fig 1G). *CTR1*-expressing SCs were also evident in stages II-VIII (Fig 1F and 1G). However, within stages IX-XII, *CTR1* staining was mostly evident on SCs and not on GCs (Fig 1H and 1I). Together, these results show that *CTR1* is expressed principally by SCs and the spermatocytes with the highest expression of *CTR1* found in the primary pachytene spermatocytes within seminiferous tubule stages II-VI. *CTR1* stage specific expression pattern in the testes of C57BL/6J mice was also evident as shown in S1C Fig.

Ctr1^{AGC} mice exhibit severe loss of germ cells with increasing age

To examine the functional significance of *CTR1* in testicular GCs, mice with a specific disruption of the *Ctr1* gene in GCs (*Ctr1*^{AGC}) were generated. *Ctr1*^{AGC} mice were examined at PND 14, 28 and 41. The *Ctr1*^{AGC} mice were indistinguishable from their WT littermates with regards to their body weight and overall appearance. However, upon examining the testis, the *Ctr1*^{AGC} mice at PND 28 and 41 had significantly reduced testicular weights as shown in Fig 2A. Similarly, significant differences in testis to body weight ratios were observed at PND 28 (a reduction of up to 60%) and PND 41 (up to 80% reduction) as compared to their WT littermates (Fig 2B). Fig 2C illustrates a marked reduction in the size of the testis of *Ctr1*^{AGC} versus WT at PND 41.

Histological evaluation of *Ctr1*^{AGC} mice testes revealed an increase in spermatogenic abnormalities with increasing age. At PND 14, WT and *Ctr1*^{AGC} testes appear similar; the first round of spermatogenesis has initiated and maturing spermatocytes (zygotene and pachytene) are present in the seminiferous tubules (Fig 2D and 2G, respectively). However, at PND 28, a degenerative seminiferous epithelium is evident in the *Ctr1*^{AGC} testes and various stages of GC subtypes were missing. In WT testis at PND 28 (Fig 2E), the most mature GC subtypes present in every seminiferous tubule were the haploid round spermatids along with elongated spermatids. Although round and elongated spermatids were present in 90% of tubules cross sections in *Ctr1*^{AGC} testis at PND 28, primary pachytene spermatocytes were either absent or present in low quantity (Fig 2H). Most of the residual GCs in PND 28 *Ctr1*^{AGC} testis had an abnormal appearance with condensed nuclei as well as SCs with large vacuoles (Fig 2H). By PND 41, when all subtypes of GCs are present in WT (Fig 2F), each tubule in the *Ctr1*^{AGC} testes were completely devoid of post-meiotic GCs with severe SC vacuolization (Fig 2I). However, the residual GCs that were present in the seminiferous tubules were mostly early stage primary

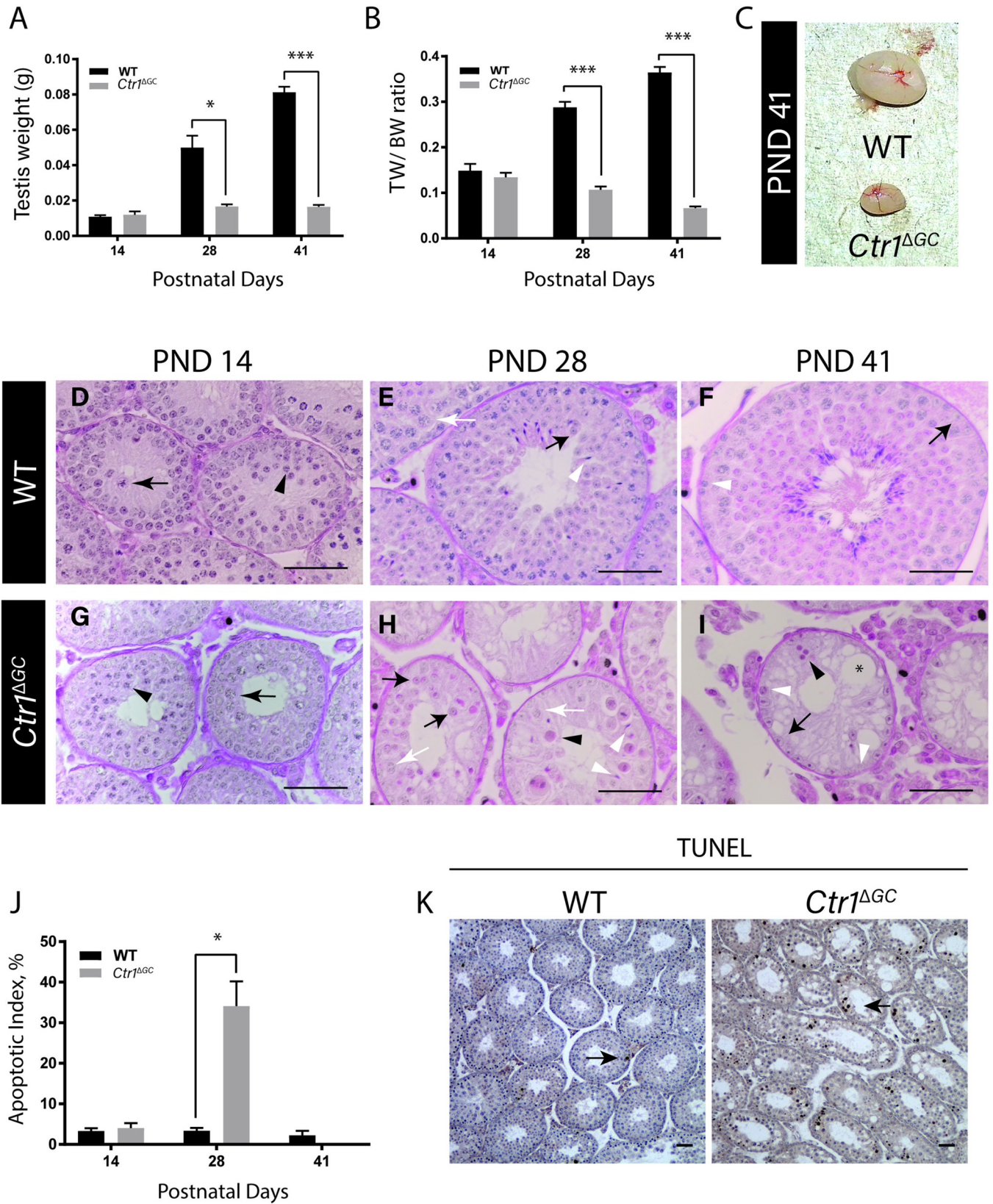


Fig 2. *Ctrl*^{AGC} mice exhibit severe loss of germ cell with increasing age. Total testis weight (A), and testis to body weight (TW/BW) ratios (B) of WT and *Ctrl*^{AGC} mice over time with a representative image of PND 41 testis (C) of both WT and *Ctrl*^{AGC} mice. (N = 3 for each age; *p < 0.05 and *** p < 0.001). Histological cross sections of WT (D, E and F) and *Ctrl*^{AGC} (G, H and I) seminiferous tubules on PND 14 (left), PND 28 (middle), and PND 41 (right) with PAS-H staining. Scale bar = 50 μ m. *Ctrl*^{AGC} testis at PND 14 (D and G) arrowhead indicating zygotene spermatocytes and arrow indicating pachytene spermatocytes. *Ctrl*^{AGC} testis at PND 28 (E and H) black arrow indicates round spermatids; white arrow indicates pachytene spermatocytes; black arrowhead indicates apoptotic GCs; white arrowhead indicates elongated spermatids. *Ctrl*^{AGC} testis at PND 41 (F and I) white arrowhead indicates residual pre-meiotic (preleptotene and spermatogonia) GCs; arrow indicates SCs; black arrowhead indicates apoptotic cells; star sign indicates SC vacuole. (J) Apoptotic index in WT or *Ctrl*^{AGC} on each PNDs (N = 3 for each age; *p < 0.05). (K) TUNEL staining indicating apoptotic cells (arrow) in the seminiferous tubules of PND 28 WT or *Ctrl*^{AGC} mice at peak apoptosis. Scale = 100 μ m.

<https://doi.org/10.1371/journal.pone.0215522.g002>

spermatocytes (e.g. preleptotene and leptotene spermatocytes) and spermatogonial cells (Fig 2I). GCs beyond leptotene stage were absent in most tubules (i.e. pachytene spermatocytes and round spermatids).

Evaluation of the incidence of GC apoptosis did not show significant differences in the apoptotic index (AI) between the genotypes (*Ctrl*^{AGC} and WT) at PND 14. The *Ctrl*^{AGC} mice at PND 28 however, displayed a surge in apoptotic GCs, with ~35% of the tubules each containing >3 TUNEL positive GCs (Fig 2J). Apoptotic GCs were found both GCs around the periphery of the tubules and surrounding the lumen (Fig 2K). By PND 41, the AI was effectively zero in the *Ctrl*^{AGC} testis, due to the near-complete loss of GCs from the seminiferous epithelium.

***Ctrl*^{AGC} testes at PND 41 contain undifferentiated spermatogonial cells with normal Sertoli cell number**

Further analysis was performed to determine whether the residual GCs in *Ctrl*^{AGC} testes at PND 41 possess proliferative activity. The mitotic activity of GCs was analyzed based on nuclear proliferating cell nuclear antigen (PCNA) staining which marks cells that are in G1 and S phase of the cell cycle and is expressed in subsets of proliferative spermatogonia and in preleptotene through pachytene spermatocytes [36]. The presence of PCNA-positive GCs in the *Ctrl*^{AGC} testes at PND 41 (Fig 3B) indicates that the GCs have maintained their mitotic activity. The overall reduced PCNA-positive cells in *Ctrl*^{AGC} testis indicates the absence of leptotene and pachytene spermatocytes in *Ctrl*^{AGC} as compared to WT, shown in Fig 3A and 3B.

The severe loss of GCs by PND 41 in *Ctrl*^{AGC} testes indicates the loss of spermatogonial stem cells (SSC). To address this possibility, we assessed the expression of transcription factor, Forkhead box protein-O1 (FOXO-1), which is involved in SSC self-renewal and expressed by undifferentiated spermatogonial cells (A_s, A_{pr} and A_{al}) [37,38]. Since these cells continually arise from SSCs, they were used as an indirect indicator of the presence of the SSC pool. Fig 3C and 3D indicates the presence of FOXO1-positive cells within the seminiferous tubules cross sections in *Ctrl*^{AGC} and WT testis at PND 41. Quantification of FOXO1-positive cells per tubule revealed no difference between *Ctrl*^{AGC} and WT testes at PND 41 (S2 Fig). To evaluate whether the numbers of SCs were altered in the testes of *Ctrl*^{AGC} mice, the numbers of cells staining positive for the SC specific marker SOX9 were evaluated. No significant changes in number of SCs per tubule were observed between the *Ctrl*^{AGC} and WT testes at PND 41 (Fig 3E).

Preliminary histological evaluation on *Ctrl*^{AGC} mice testes at PND 70 indicated a lack of regeneration of spermatogenesis, as shown in Fig 3F. Seminiferous tubules of *Ctrl*^{AGC} testis displayed clusters of SCs that protruded into the lumen, a symptom of prolonged SC inactivity due to loss of GCs found in testes of sterile mice [39] (Fig 3F and 3G). However, similar to *Ctrl*^{AGC} testis observed at PND 41, the *Ctrl*^{AGC} testes at PND 70 did contain FOXO-1 positive spermatogonia (Fig 3H).

***Ctrl*^{ASC} mice at PND 60 are indistinguishable from WT littermates**

To examine whether loss of CTR1 expression in SC would also affect spermatogenesis, mice with a specific disruption of the *Ctrl* gene in SC (*Ctrl*^{ASC}) were generated. The specific

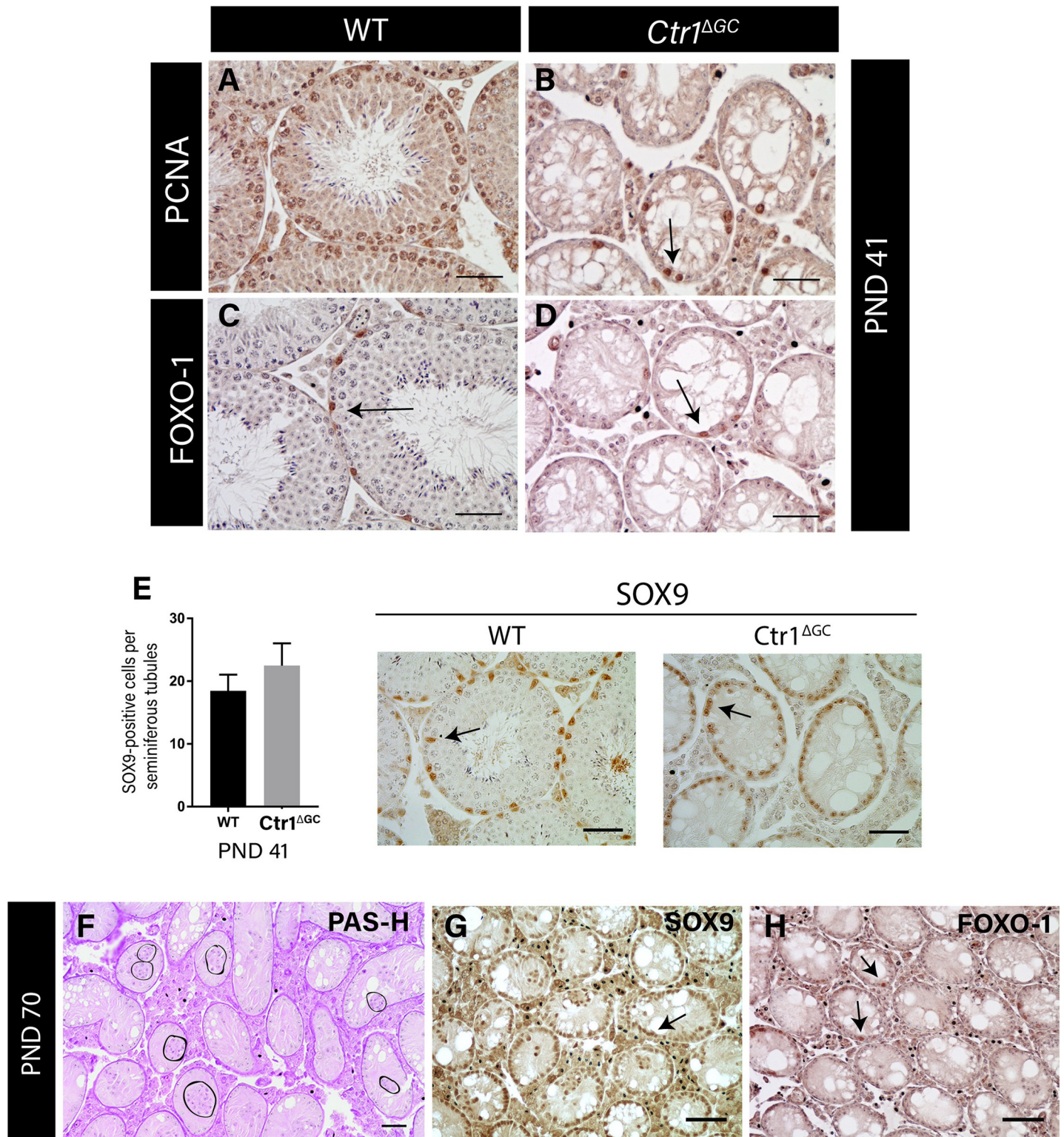


Fig 3. *Ctrl*^{ΔGC} mice at PND 41 display presence of undifferentiated spermatogonial cells and normal number of Sertoli cells in adult testes of *Ctrl*^{ΔGC} mice. Immunohistochemical nuclear staining for PCNA in GCs of both (A) WT and (B) *Ctrl*^{ΔGC} testes. Presence of FOXO-1 expressing undifferentiated spermatogonial cells at PND 41 in (C) WT and (D) *Ctrl*^{ΔGC} testes. Average number of SOX9-positive cells per seminiferous tubules (E). On right, representative immunohistochemical staining from SOX9 analysis of WT and *Ctrl*^{ΔGC}; arrows indicating SOX9-positive SCs (Average ±SD, N = 3 for each genotype). Scale bar = 100 μm. Histological analysis on *Ctrl*^{ΔGC} testis at PND 70 indicating multiple clusters of SCs in the lumen indicated by circles (F) with PAS-H staining. SOX9-positive SCs clarifying the SCs clusters in the lumen (G). (H) Presence of FOXO-1-positive spermatogonial cells, indicated by arrows, within the tubules of *Ctrl*^{ΔGC} testis at PND 70. Scale = 50 μm.

<https://doi.org/10.1371/journal.pone.0215522.g003>

knockout of *Ctrl* gene by the SCs was verified by immunohistochemical staining in testis cross sections of WT and *Ctrl*^{ASC} mice. Fig 4A indicates the localization of CTR1 on both on primary spermatocytes and on SCs in the WT testis, whereas CTR1 is localized only on primary spermatocytes within the seminiferous tubules of the *Ctrl*^{ASC} testis (Fig 4C). To further verify the knockout of *Ctrl* in SCs, *Ctrl* gene and protein expression of isolated SCs from both WT and *Ctrl*^{ASC} mice were compared using q-PCR and immunoblotting. Fig 4E indicates a 70% reduced in *Ctrl* mRNA expression by *Ctrl*^{ASC} SCs compared to WT SCs. Protein expression of CTR1 in crude membrane extracts of isolated SCs from *Ctrl*^{ASC} mice was undetectable compared to WT mice (Fig 4F). Similarly, testis histology of *Ctrl*^{ASC} mice at earlier age (PND 14) was observed to be comparable to their WT littermates (S3A and S3B Fig).

The *Ctrl*^{ASC} mice displayed similar appearance as their WT littermates; no obvious behavioral deficit was noted. Testes weight, testes to body weight ratio, and testicular spermatid head counts of both *Ctrl*^{ASC} and WT mice were comparable at PND 60 as indicated in Fig 4G. The *Ctrl*^{ASC} had similar numbers of SCs as their WT littermates shown in Fig 4H and 4I. When *Ctrl*^{ASC} males were crossed with WT females to assess fertility, normal length of conception and number of pups was observed in *Ctrl*^{ASC} male mice (average litter size 9 ± 1) compared to WT male mice (average litter size 9).

***Ctrl*^{ASC} mice exhibit testicular copper deficiency**

Since *Ctrl*^{ASC} mice exhibited normal fertility, further experiments were carried out to examine whether CTR1 in SCs is involved in Cu homeostasis in the testis. The Cu concentration of *Ctrl*^{ASC} mice testis displayed up to 30% reduced steady-state Cu levels compared to their WT littermates (Fig 5A). The Cu levels were further analyzed within the seminiferous tubules, which include both GCs and SCs. The *Ctrl*^{ASC} mice displayed up to 40% reduced Cu levels compared to WT as shown in Fig 5B. To examine whether reductions in the steady-state levels of Cu had any effect on other metals, iron and zinc were evaluated in testes and seminiferous tubules, but no differences were observed (Fig 5A and 5B).

Based on reduced testicular steady-state Cu levels in *Ctrl*^{ASC} mice, we examined whether these changes affected Cu-dependent enzyme activities or cellular regulations. Cu-chaperone for superoxide dismutase (CCS) protein captures and supplies Cu to the Cu, Zn-superoxide dismutase (SOD1) enzyme and reduction in Cu levels have been shown to cause up-regulation of CCS, hence CCS protein levels are inversely proportional to their intracellular Cu bioavailability [40]. Indeed, *Ctrl*^{ASC} testes exhibited elevated ($p = 0.0656$) protein level of steady-state CCS compared to WT, indicating testicular Cu deficiency (Fig 5C and 5D). Further analysis was performed on the cuproenzyme cytochrome c oxidase (CCO), which is the fourth complex of the respiratory chain reaction within the mitochondria that requires Cu for the assembly of the subunits within complex 4 [41]. The CCO activity and protein expression of the testis from both genotypes were assessed. As predicted, *Ctrl*^{ASC} testes exhibited up to 60% reduction in CCO activity compared to WT testes (Fig 5E). Consistent with the reduced CCO activity, COX5A, a CCO complex subunit, protein levels were also reduced in *Ctrl*^{ASC} testes as compared to WT testes, as shown in Fig 5F.

Loss of CTR1 in Sertoli cells display normal copper levels but copper deficient phenotype

Since whole testis and seminiferous tubules displayed a Cu deficient status, we further examined Cu levels in primary SCs derived from immature (PND 25) *Ctrl*^{ASC} and WT mice testes. Intracellular Cu levels was measured using ICP-MS on primary SC of WT and *Ctrl*^{ASC} mice. Surprisingly, Cu levels in *Ctrl*^{ASC} SCs were similar to Cu levels in WT SCs as indicated in Fig 6A. However, SCs of *Ctrl*^{ASC} mice displayed almost two-fold increase in CCS protein levels

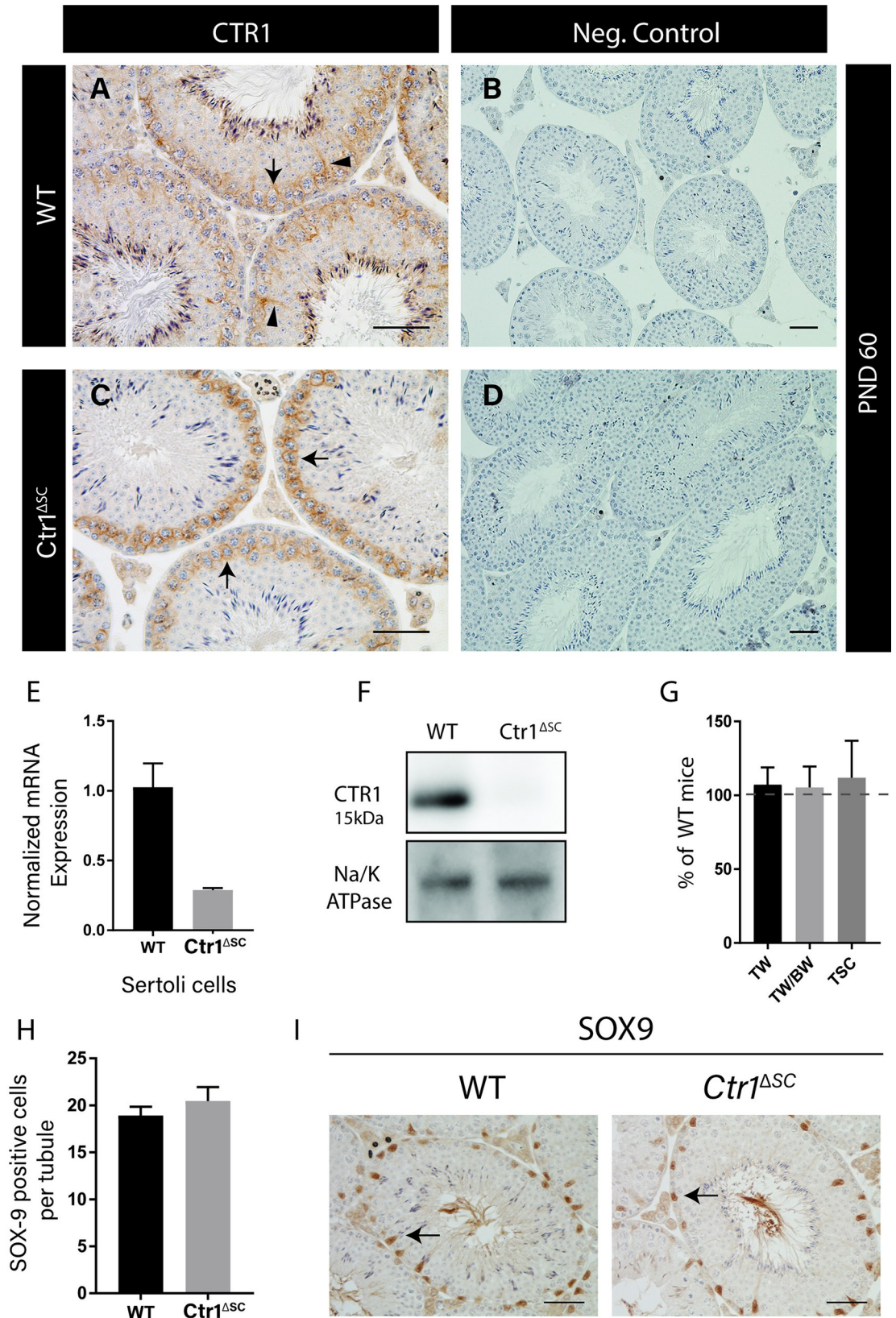


Fig 4. *Ctr1*^{ASC} mice at PND 60 are indistinguishable from WT littermates. Immunohistochemical analysis of CTR1 protein expression within the *Ctr1*^{ASC} and WT testis. (A) CTR1 localization on within the seminiferous tubules in WT mice expressed on the SCs (arrowheads) and spermatocytes (arrow), and CTR1 localization on the spermatocytes only (arrows) in the *Ctr1*^{ASC} testis (C). Negative secondary only control of WT and *Ctr1*^{ASC} testis shown on the right (B and D, respectively). (E) Q-PCR on *Ctr1* mRNA expression normalized to *Hprt1* gene indicates up to 70% reduced expression in *Ctr1*^{ASC} SCs compared to WT (average \pm SEM). (F) Immunoblot analysis on crude membrane extract on WT and *Ctr1*^{ASC} SC isolates against CTR1 antibody shows undetectable CTR1 expression in *Ctr1*^{ASC} compared to WT mice. (G) Testicular weight (TW), testes to body weight ratio (TW/BW) and testicular spermatid head counts (TSC) all displayed similar to their WT littermates. The graph represents relative measurements of *Ctr1*^{ASC} mice compared to WT mice, dashed line represents 100% of each measurement in WT mice (average \pm SD). (H) SOX9-positive cells within the seminiferous tubules of both WT and *Ctr1*^{ASC} testes displayed similar number of SCs. (I) Representative images of SOX9 staining indicated by arrows in both WT and *Ctr1*^{ASC} testis. Each data point is representative of 4–5 mice of each genotype. Scale bar = 100 μ m.

<https://doi.org/10.1371/journal.pone.0215522.g004>

when compared to SCs of WT mice as shown in Fig 6B and 6C. Similarly, SCs of *Ctr1*^{ASC} mice exhibited a 45% reduced CCO enzyme activity and reduced protein expression of COX5A as compared to SCs of WT mice (Fig 6D and 6E) indicating lower Cu bioavailability as compared to the WT SCs even though intracellular Cu levels were similar to WT.

Discussion

The expression pattern of the *Ctr1* gene and protein has been demonstrated in mice testis, but the physiological significance of CTR1 localization within the cell types of seminiferous tubules has not been identified [15,22]. In order to interrogate and differentiate the physiological significance of CTR1 protein in functional spermatogenesis, we developed and characterized both GC-specific (*Ctr1*^{AGC}) and SC-specific (*Ctr1*^{ASC}) *Ctr1* knockout mice.

Primary spermatocytes are in meiotic prophase I which go through series of morphological transition phases, starting from pre-leptotene, leptotene, zygotene, pachytene, and diplotene spermatocytes [9]. The high localization of CTR1 on pachytene spermatocytes implies that precise levels of Cu are needed for spermatocytes to progress through meiotic prophase I, as observed in yeast and *Drosophila* models [19,21]. The reason why CTR1 is specifically expressed at pachytene stage is not clear. However, it may reflect the high energy demand and mitochondrial biogenesis that occurs during meiosis. Mammalian testes have a series of testis-specific mitochondrial protein subunits that are expressed in GCs [42,43]. Cytochrome-c oxidase (CCO) is ubiquitously expressed, however in mammalian testes, the CCO subunit II, which contains the Cu binuclear binding sites, are highly expressed in pachytene spermatocytes [44]. Interestingly, a testis-specific cytochrome c (cyt c) is predominantly expressed in zygotene and pachytene spermatocytes which is believed to have a distinct role in GC mitochondria that is different from that of somatic cyt c in that it interacts with the testis-specific CCO enzyme [43–46]. Therefore, the expression and regulation of the cell type-specific mitochondrial proteins may underscore the specific localization of CTR1 on pachytene spermatocytes.

Using the *Ctr1*^{AGC} mice model, we demonstrated physiological evidence that CTR1 is required in GCs for the establishment of functional spermatogenesis during puberty (PND28). At PND 14 the *Ctr1*^{AGC} testis displays a phenotype indistinguishable from that of the WT littermates with the presence of early stages of primary spermatocytes [9]. In mice, the process of a SSCs to produce elongated spermatids take 35 days [9,47]. At PND 28, the presence of round spermatids, but lack of primary pachytene spermatocytes in *Ctr1*^{AGC} tubules suggest that the first round of spermatogenesis has occurred leading to production of spermatids, but the subsequent cycle has failed to complete; resulting in seminiferous tubules that are almost devoid of later stages of spermatocytes and spermatids by PND 41 and in older mice (PND70). The presence of early spermatocytes (preleptotene and leptotene), PCNA- and FOXO-1-positive

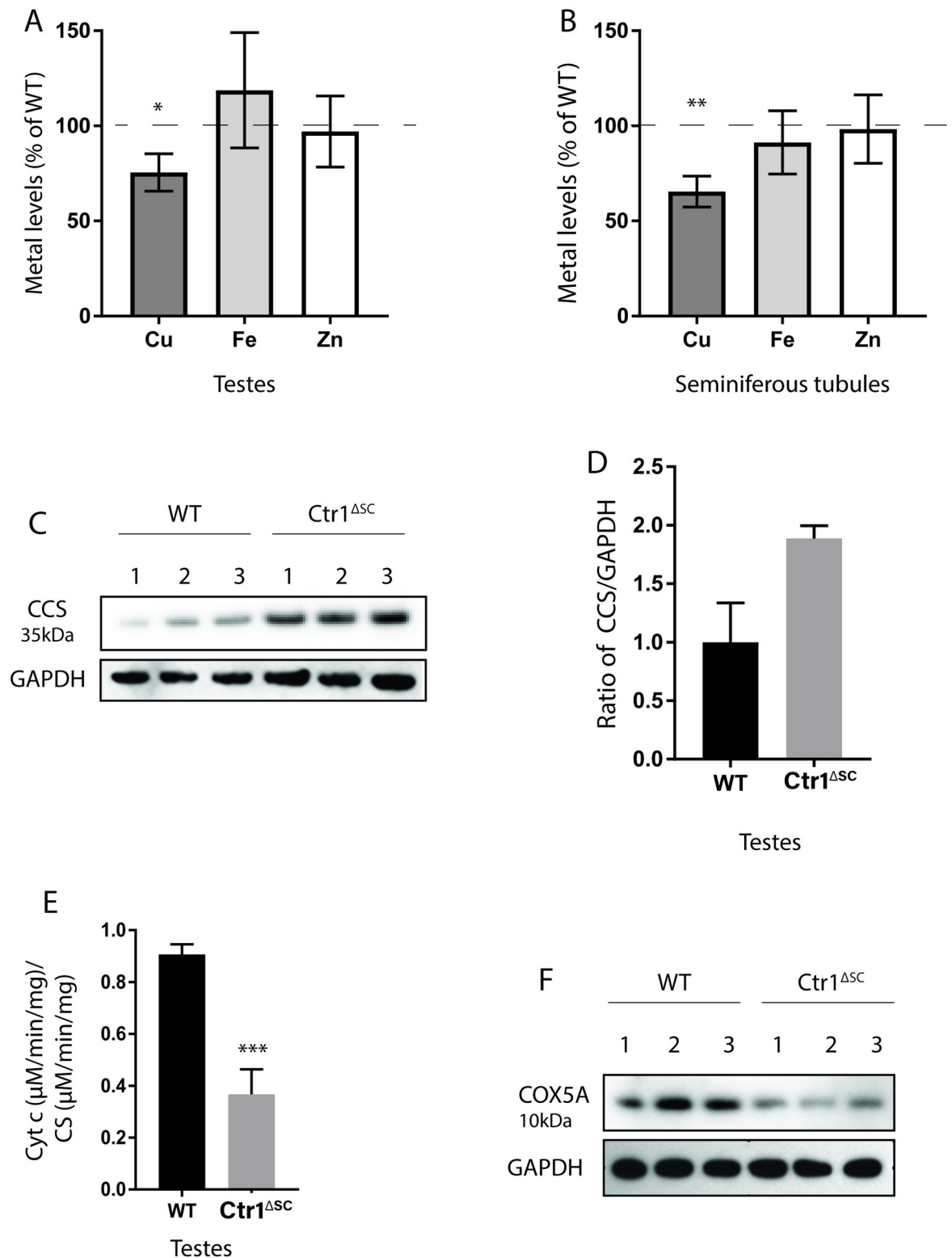


Fig 5. *Ctr1*^{ΔSC} mice exhibit testicular copper deficiency. (A) Relative Cu, Fe and Zn levels in *Ctr1*^{ΔSC} testis and in (B) *Ctr1*^{ΔSC} seminiferous tubules compared to WT testis. Data represent percent concentration (μg/g dry tissue weight) of *Ctr1*^{ΔSC} tissues compared to WT tissues (average ±SD). Dashed line represents 100% of each metal in WT tissues. For each genotype N = 4–5, *P<0.05, **p<0.005. (C) Immunoblot analysis on CCS and GAPDH is shown as loading control. Three animals were randomly selected and analyzed from each WT and *Ctr1*^{ΔSC} mice. Each number above represents an animal from each genotype. (D) Quantified protein expression of CCS

normalized to GAPDH expression (average \pm SEM, $N = 3$, $p = 0.0656$). (E) Cytochrome c oxidase (CCO) activity of WT and *Ctr1*^{ASC} testis. Tissue lysates from randomly selected three WT and *Ctr1*^{ASC} mice were analyzed to measure CCO activity. Graph represents the rate of cytochrome c (cyt c) oxidation ($\mu\text{M}/\text{min}/\text{mg}$ of protein lysate) of *Ctr1*^{ASC} and WT testis and normalized to citrate synthase (CS) activity for each sample (average \pm SD, $N = 3$, $***p < 0.001$). (F) Immunoblot analysis on the COX5A, a CCO complex subunit, and GAPDH is shown as loading control.

<https://doi.org/10.1371/journal.pone.0215522.g005>

cells in most tubule cross section of the *Ctr1*^{AGC} testis indicate that the proliferative and undifferentiated spermatogonia are still being generated from SSC pool, however the progression of spermatogenesis beyond leptotene stage of GC development is lost. In align with what previously discussed, Nakada et. al. group observed similar phenotype in adult mice (PND >100) with severe mitochondrial respiratory defects exhibit meiotic arrest at zygotene stage and enhanced apoptosis. Although our analysis on spermatocyte subtypes is based on histological assessment of the seminiferous tubule cross sections, further and more detailed analysis on spermatocyte stages can illustrate whether CTR1-dependent Cu import in GCs is essential for mitochondrial respiratory activity for the progression to the pachytene stages during meiosis.

These observations, along with the stage-specific expression of CTR1 on pachytene spermatocytes support the notion that the spermatogenic defect occurs after the first round of spermatogenesis and arrests prior to pachytene stage of meiosis. Why the early phase of first round of spermatogenesis appears to occur normally remains unclear, but could indicate that the requirement for Cu transport is age dependent. In support of this notion, testicular concentration of Cu varies with age; male mice have low levels at PND ~7 which increases to peak levels by PND 20, and then declines through PND ~180 [22,48]. Whether Cu supplementation can rescue the *Ctr1*^{AGC} mice phenotype requires further investigation which would determine if the spermatogenic failure is due to the age specific role of CTR1 in Cu absorption or perhaps due to a yet appreciated function of the CTR1 protein in GC development in mice. Given the conserved function of *Ctr1* in eukaryotes, Streiger et al reported that the male sterility with loss of *Ctr1C* was rescued with Cu supplementation. The presence of spermatogonial cells in adult *Ctr1*^{AGC} mice provides the possibility of spermatogenic recovery in *Ctr1*^{AGC} mice by Cu supplementation to be plausible.

Functional spermatogenesis is highly dependent on the support system of the neighboring somatic SCs. SCs are polarized epithelial cells that function to ensure a suitable microenvironment for spermatogenesis to take place by regulating the secretion and transportation of essential ions and metabolites to the developing GCs [10]. As we have demonstrated, CTR1 is predominantly localized on the primary pachytene spermatocytes which are located in the adluminal compartment within the BTB. This observation suggested that the source of Cu in the adluminal compartment may be, in part, from the SCs, and that the CTR1 expression by SCs may play a role in functional spermatogenesis. To test this hypothesis, *Ctr1*^{ASC} mice were generated. Unexpectedly, *Ctr1*^{ASC} mice testes exhibited comparable spermatogenesis and fertility as their WT littermates suggesting that the CTR1 expression in SCs is dispensable for normal spermatogenesis to occur. However, the overall reduced Cu levels and Cu-dependent protein activity and expression in both the whole testis and in the seminiferous tubules, suggests that CTR1 in SCs does function, at least, partly in Cu transport in testis. Given that deletion of *Ctr1* in GCs manifest defects in GC development, the importance of Cu delivery for GCs may have exerted the SCs to develop compensatory or a separate Cu acquisition pathway to provide essential supply of Cu for the GCs. This is evident in that only a 30% reduction in Cu level and 60% reduction in CCO activity were observed in the testis of *Ctr1*^{ASC} mice, and that *Ctr1*^{ASC} mice were able to sire pups. Normal spermatogenesis observed in *Ctr1*^{ASC} mice despite the reduced testicular Cu level contradicts with previous reports that have documented impairment of testicular function in Cu deficient animals [6–8]. Although the testicular Cu

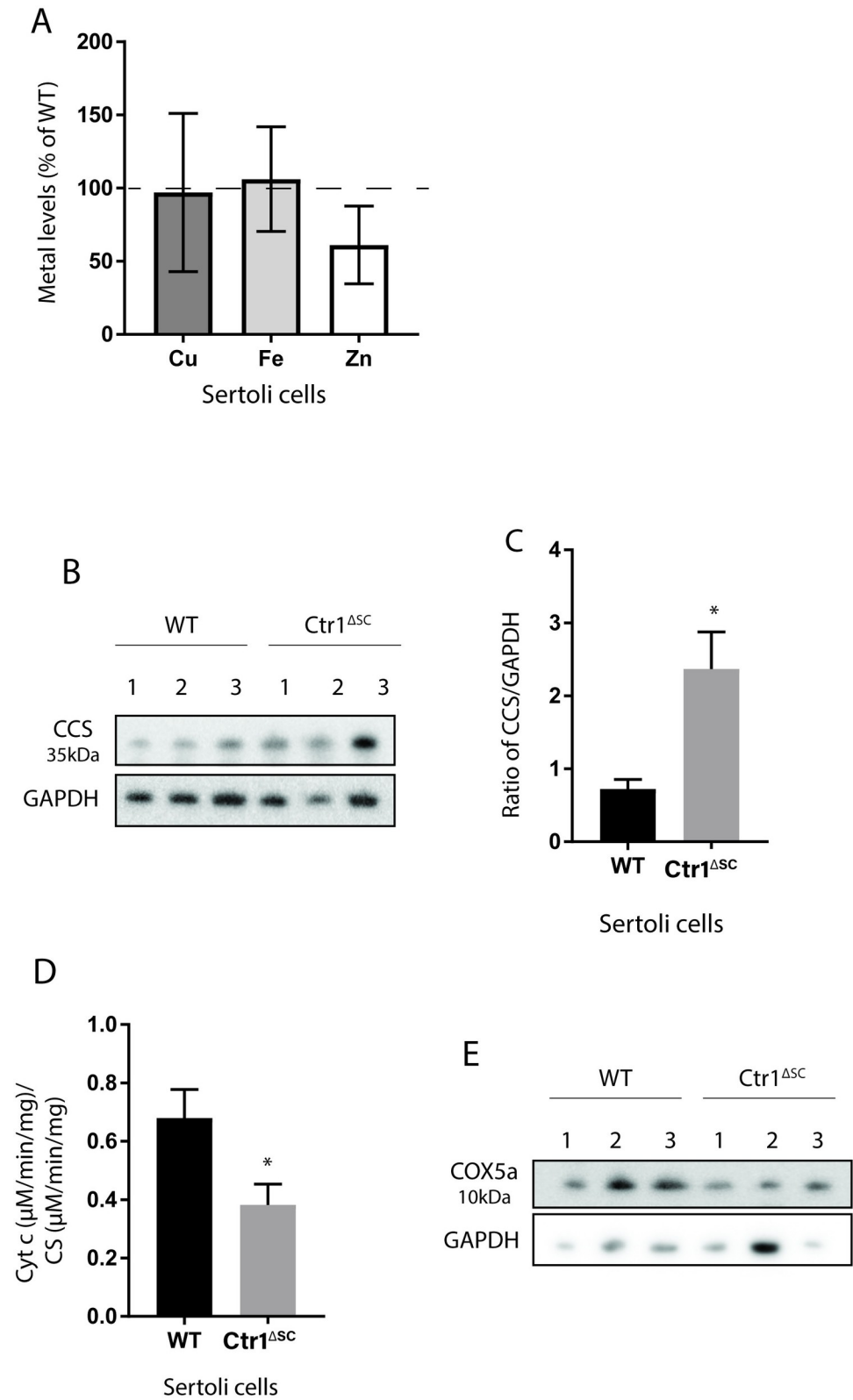


Fig 6. Loss of CTR1 in Sertoli cells display normal copper levels but copper deficient phenotype. (A) Relative Cu, Fe and Zn levels in primary SCs isolated from WT and *Ctr1*^{ΔSC} testes. Data represents percent concentration (μg of metal per 10,000 cells) of *Ctr1*^{ΔSC} SCs compared to WT SCs. Dashed line represents 100% of each metal in WT SCs.

(average \pm SD, N = 5–7). (B) Immunoblot analysis (C) quantified protein expression of CCS normalized to GAPDH expression. Primary SCs isolated from three animals analyzed from each WT and *Ctr1*^{ASC} mice (average \pm SEM, N = 3, *p<0.05). (D) CCO activity of WT and *Ctr1*^{ASC} primary SCs. Cell lysates from three different WT and *Ctr1*^{ASC} mice were analyzed to measure CCO activity. Graph represents the rate of cyt c oxidation (μ M/min/mg of protein lysate) of WT and *Ctr1*^{ASC} SCs and normalized CS activity for each sample (average \pm SD, N = 3, *p<0.05). (E) Immunoblot analysis on the COX5A expression of primary SCs derived from three individual mice from each genotype. GAPDH is shown as loading control.

<https://doi.org/10.1371/journal.pone.0215522.g006>

level was not stated in these studies, this discrepancy can be due to the systemic Cu deficiency in animals rather than tissue/cell specific Cu deficiency. Our analysis on the fertility of the *Ctr1*^{ASC} mice is limited on testicular spermatid head count thus we cannot rule out the possibility that loss of CTR1 in SCs affects sperm quality in these mice as a secondary effect. Nevertheless, *Ctr1*^{ASC} mice sired comparable number of pups when mated with virgin WT females as to WT males.

Interestingly, *in vitro* analysis of intracellular Cu levels of primary SCs derived from WT and *Ctr1*^{ASC} mice displayed comparable levels of Cu even though SCs of *Ctr1*^{ASC} mice exhibited Cu deficient phenotype. CTR1 protein has been shown to localize both on plasma membrane and on intracellular vesicles, depending on the cell type [25,49]. It is demonstrated on previous reports that CTR1 is involved in both importing extracellular Cu, as well as importing Cu from endosomal compartment [49]. Therefore, these observations may suggest that perhaps CTR1 in SCs mainly functions in mobilizing Cu from intracellular vesicle, which could explain why the SCs in *Ctr1*^{ASC} display a deficiency in Cu that is biologically unavailable. The possibility of compensatory Cu acquisition mechanism affecting Cu levels in cultured primary SCs cannot be ignored. However, given that *Ctr1*^{ASC} testis had 30% reduction in Cu level, together suggest that there may be an alternative Cu acquisition system that partially complements CTR1-dependent Cu uptake pathway. A second Cu transporter, CTR2 (SLC31A2), which is structurally related to CTR1 protein, has been reported to express high levels in testis [17]. CTR2 functions as a low affinity Cu importer, Cu exporter from intracellular vesicle to cytoplasm, and as a regulator of macropinocytosis, [50–52] and thus it could play a role in Cu acquisition with loss of CTR1 in SCs both *in vivo* and *in vitro*.

Reduced Cu levels in testis and in seminiferous tubules, but not in SCs, suggests the possibility that CTR1 in SCs functions in efficiently transporting or mobilizing Cu from basolateral compartment to the adluminal compartment of the SCs to supply the GCs, which can explain the stage specific localization of CTR1 in SCs along the basal and adluminal compartment of the seminiferous tubules. A similar observation was made in mice with intestinal epithelial cell-specific *Ctr1* knockout [25]. These mice exhibited Cu accumulation in enterocytes even though the intestinal epithelial cells itself and other peripheral organs displayed Cu deficiency, demonstrating another role of CTR1 in mobilizing Cu from the intracellular vesicle to other organelles and subsequently to the peripheral organs [17,25]. Therefore, it is possible that with loss of CTR1 in SCs, Cu is held in SCs that may not be biologically available and that Cu deficiency observed in testis and in seminiferous tubules may be primarily due to Cu deficiency in GCs. Alternatively, CTR1 in SCs may function in Cu uptake that is released from GCs, in order to protect GCs from Cu overload, or recycle Cu back to the primary spermatocytes, a pathway analogous to how iron is recycled and maintained within the seminiferous tubules [53]. However, given that the testis and seminiferous tubules of *Ctr1*^{ASC} mice exhibited significant Cu deficiency, may not support the latter theory.

In summary, we have demonstrated for the first time, the differential physiological significance of CTR1 in two different testicular cell types, GCs and SCs. The high expression of CTR1 on pachytene spermatocytes and the progressive failure of spermatogenesis in adult

Ctr1^{ΔGC} mice, points to the critical requirement of CTR1 for mammalian spermatogenesis. In contrast, the loss of expression of CTR1 in SCs did not negatively affect spermatogenesis even though the testis of these mice exhibited a significant reduction in Cu. Taken together, these observations support the hypothesis that CTR1 protein expression is required for GC development and functional spermatogenesis.

Supporting information

S1 Fig. (A) Breeding strategies for generating GC specific (*Ddx4-Cre*) and SC specific (*Amh-Cre1*) knockout mice. A schematic depiction of alleles encoding for *Ctr1* gene. White box represents *Ctr1* structural gene, grey triangle represents loxP sites flanking the *Ctr1* gene. Cre recombinase gene under the *Ddx4* or *Amh* or promoter gene is represented as black and white box, where white is Cre recombinase gene and black is promoter gene. Initially, homozygous *Ctr1*^{fl/fl} female mice were crossed with male mice carrying either *Ddx4-Cre* or *Amh-Cre* gene with WT *Ctr1*^{+/+} genotype. The heterozygous male mice carrying either *Ddx4-Cre; Ctr1*^{+/fl} or *Amh-Cre; Ctr1*^{+/fl} genotype from the initial cross were then back-crossed to *Ctr1*^{fl/fl} female mice to obtain GC (*Ddx4-Cre; Ctr1*^{fl/Δ}, *Ctr1*^{ΔGC}) or SC specific (*Amh-Cre; Ctr1*^{fl/Δ}, *Ctr1*^{ΔSC}) *Ctr1* knockout mice. (B) Representative PCR genotyping results showing mouse tail DNA samples with WT (*Ctr1*^{+/+}), heterozygous floxed (*Ctr1*^{fl/+}), and homozygous floxed mouse (*Ctr1*^{fl/fl}). (C) Immunohistochemical analysis of stage specific CTR1 protein expression in adult C57BL/6J testes cross section. Arrows indicates CTR1 on pachytene spermatocytes. Arrowheads indicate CTR1 on SCs.

(PDF)

S2 Fig. Graph showing average number of FOXO1-positive cells per tubules (calculating based on the total number of tubules analyzed). For each animal/genotype ≥ 100 tubules were counted.

(PDF)

S3 Fig. Histological cross section of WT (A) and *Ctr1*^{ΔSC} (B) mice testis at PND 14. Scale = 180 μ m.

(PDF)

Acknowledgments

We are grateful to Dr. Dennis Thiele for providing the *Ctr1*^{fl/+} mice and CTR1 antibody. We thank Dr. Nathaniel Miller (Jackson School of Geosciences, University of Texas, Austin) for performing all inductively coupled plasma-mass spectrometry assays reported in this manuscript. We appreciate Dr. Pei-Li Yao's excellent assistance in staging CTR1 expression in the mice testes. We would also like to thank Jorine Voss, Richa Tiwary and Ross Gillette for their critical reading this manuscript, and Angela Stermer and Caitlin Murphy for their helpful advice.

Author Contributions

Conceptualization: Rashin Ghaffari, Kristin R. Di Bona, John H. Richburg.

Data curation: Rashin Ghaffari, Kristin R. Di Bona, Christopher L. Riley.

Formal analysis: Rashin Ghaffari, Christopher L. Riley.

Funding acquisition: John H. Richburg.

Investigation: Rashin Ghaffari, John H. Richburg.

Methodology: Rashin Ghaffari.

Project administration: John H. Richburg.

Resources: John H. Richburg.

Supervision: John H. Richburg.

Writing – original draft: Rashin Ghaffari, John H. Richburg.

Writing – review & editing: Rashin Ghaffari, John H. Richburg.

References

1. Peña MM, Lee J, Thiele DJ. A delicate balance: homeostatic control of copper uptake and distribution. *J Nutr.* 1999; 129: 1251–1260. <https://doi.org/10.1093/jn/129.7.1251> PMID: 10395584
2. Tapiero H, Townsend DM, Tew KD. Trace elements in human physiology and pathology. *Copper. Bio-medicine & Pharmacotherapy.* 2003; 57: 386–398. [https://doi.org/10.1016/S0753-3322\(03\)00012-X](https://doi.org/10.1016/S0753-3322(03)00012-X)
3. Prohaska JR. Impact of copper deficiency in humans. *Ann NY Acad Sci.* 2014; 1314: 1–5. <https://doi.org/10.1111/nyas.12354> PMID: 24517364
4. Kim B-E, Nevitt T, Thiele DJ. Mechanisms for copper acquisition, distribution and regulation. *Nat Chem Biol.* 2008; 4: 176–185. <https://doi.org/10.1038/nchembio.72> PMID: 18277979
5. Roychoudhury S, Nath S, Massanyi P, Stawarz R, Kacaniova M, Kolesarova A. Copper-induced changes in reproductive functions: in vivo and in vitro effects. *Physiol Res.* 2016; 65: 11–22. PMID: 26596322
6. Lyubimov AV, Smith JA, Rousselle SD, Mercieca MD, Tomaszewski JE, Smith AC, et al. The effects of tetrathiomolybdate (TTM, NSC-714598) and copper supplementation on fertility and early embryonic development in rats. *Reproductive Toxicology.* 2004; 19: 223–233. <https://doi.org/10.1016/j.reprotox.2004.07.006> PMID: 15501388
7. Aupperle H, Schoon HA, Frank A. Experimental copper deficiency, chromium deficiency and additional molybdenum supplementation in goats—pathological findings. *Acta Vet Scand.* 2001; 42: 311–321. <https://doi.org/10.1186/1751-0147-42-311> PMID: 11887391
8. Van Niekerk FE, Van Niekerk CH. The influence of experimentally induced copper deficiency on the fertility of rams. I. Semen parameters and peripheral plasma androgen concentration. *J S Afr Vet Assoc.* 1989; 60: 28–31. PMID: 2724283
9. Griswold MD. Spermatogenesis: The Commitment to Meiosis. *Physiol Rev.* 2015; 96: 1–17. <https://doi.org/10.1152/physrev.00013.2015> PMID: 26537427
10. Cheng CY, Mruk DD. The Blood-Testis Barrier and Its Implications for Male Contraception. *Pharmacological Reviews.* 2011; 64: 16–64. <https://doi.org/10.1124/pr.110.002790> PMID: 22039149
11. Su L, Mruk DD, Cheng CY. Drug transporters, the blood-testis barrier and spermatogenesis. *Journal of Endocrinology.* 2010; 1–17. <https://doi.org/10.1677/JOE-10-0363> PMID: 21134990
12. Nevitt T, Öhrvik H, Thiele DJ. Charting the travels of copper in eukaryotes from yeast to mammals. *Biochimica et Biophysica Acta (BBA)—Molecular Cell Research.* 2012; 1823: 1580–1593. <https://doi.org/10.1016/j.bbamcr.2012.02.011> PMID: 22387373
13. Dancis A, Haile D, Yuan DS, Klausner RD. The *Saccharomyces cerevisiae* copper transport protein (Ctr1p). Biochemical characterization, regulation by copper, and physiologic role in copper uptake. *J Biol Chem. American Society for Biochemistry and Molecular Biology;* 1994; 269: 25660–25667. PMID: 7929270
14. Lee J, Prohaska JR, Dagenais SL, Glover TW, Thiele DJ. Isolation of a murine copper transporter gene, tissue specific expression and functional complementation of a yeast copper transport mutant. *Gene.* 2000; 254: 87–96. PMID: 10974539
15. Kuo YM, Zhou B, Cosco D, Gitschier J. The copper transporter CTR1 provides an essential function in mammalian embryonic development. *Proc Natl Acad Sci USA. National Acad Sciences;* 2001; 98: 6836–6841. <https://doi.org/10.1073/pnas.111057298> PMID: 11391004
16. Cottignoli S. Expression and cellular localization of Copper transporter 2 (Ctr2) in *Mus musculus*. 2009. <https://doi.org/10.6092/unibo/amsdottorato/1883>
17. Öhrvik H, Nose Y, Wood LK, Kim B-E, Gleber S-C, Ralle M, et al. Ctr2 regulates biogenesis of a cleaved form of mammalian Ctr1 metal transporter lacking the copper- and cisplatin-binding ecto-domain. *Proc*

- Natl Acad Sci USA. National Academy of Sciences; 2013; 110: E4279–88. <https://doi.org/10.1073/pnas.1311749110> PMID: 24167251
18. Lee J, Prohaska JR, Thiele DJ. Essential role for mammalian copper transporter Ctr1 in copper homeostasis and embryonic development. *Proc Natl Acad Sci USA. National Acad Sciences*; 2001; 98: 6842–6847. <https://doi.org/10.1073/pnas.111058698> PMID: 11391005
 19. Beaudoin J, Ekici S, Daldal F, Ait-Mohand S, Guérin B, Labbé S. Copper transport and regulation in *Schizosaccharomyces pombe*. *Biochim Soc Trans*. 2013; 41: 1679–1686. <https://doi.org/10.1042/BST2013089> PMID: 24256274
 20. Beaudoin J, Ioannoni R, López-Maury L, Bähler J, Ait-Mohand S, Guérin B, et al. Mfc1 is a novel forespore membrane copper transporter in meiotic and sporulating cells. *J Biol Chem. American Society for Biochemistry and Molecular Biology*; 2011; 286: 34356–34372. <https://doi.org/10.1074/jbc.M111.280396> PMID: 21828039
 21. Steiger D, Fetchko M, Vardanyan A, Atanesyan L, Steiner K, Turski ML, et al. The *Drosophila* copper transporter Ctr1C functions in male fertility. *J Biol Chem. American Society for Biochemistry and Molecular Biology*; 2010; 285: 17089–17097. <https://doi.org/10.1074/jbc.M109.090282> PMID: 20351114
 22. Ogórek M, Lenartowicz M, Starzyński R, Jończy A, Staroń R, Doniec A, et al. Atp7a and Atp7b regulate copper homeostasis in developing male germ cells in mice. *Metallomics. The Royal Society of Chemistry*; 2017; 9: 1288–1303. <https://doi.org/10.1039/c7mt00134g> PMID: 28820536
 23. Gallardo T, Shirley L, John GB, Castrillon DH. Generation of a germ cell-specific mouse transgenic Cre line, Vasa-Cre. *Genesis*. 2007; 45: 413–417. <https://doi.org/10.1002/dvg.20310> PMID: 17551945
 24. Lécureuil C, Fontaine I, Crepieux P, Guillou F. Sertoli and granulosa cell-specific Cre recombinase activity in transgenic mice. *Genesis*. 2002; 33: 114–118. <https://doi.org/10.1002/gene.10100> PMID: 12124943
 25. Nose Y, Kim B-E, Thiele DJ. Ctr1 drives intestinal copper absorption and is essential for growth, iron metabolism, and neonatal cardiac function. *Cell Metabolism*. 2006; 4: 235–244. <https://doi.org/10.1016/j.cmet.2006.08.009> PMID: 16950140
 26. Sawhney P, Giammona CJ, Meistrich ML, Richburg JH. Cisplatin-induced long-term failure of spermatogenesis in adult C57/BL/6J mice. *Journal of Andrology*. 2005; 26: 136–145. PMID: 15611578
 27. Harman JG, Richburg JH. Cisplatin-induced alterations in the functional spermatogonial stem cell pool and niche in C57/BL/6J mice following a clinically relevant multi-cycle exposure. *Toxicology Letters. Elsevier Ireland Ltd*; 2014; 227: 99–112. <https://doi.org/10.1016/j.toxlet.2014.03.019> PMID: 24704392
 28. Lee J, Richburg JH, Younkin SC, Boekelheide K. The Fas system is a key regulator of germ cell apoptosis in the testis. *Endocrinology*. 1997; 138: 2081–2088. <https://doi.org/10.1210/endo.138.5.5110> PMID: 9112408
 29. Karzai AW, Wright WW. Regulation of the synthesis and secretion of transferrin and cyclic protein-2/cathepsin L by mature rat Sertoli cells in culture. *Biology of Reproduction*. 1992; 47: 823–831. PMID: 1477208
 30. Gong Z-K, Wang S-J, Huang Y-Q, Zhao R-Q, Zhu Q-F, Lin W-Z. Identification and validation of suitable reference genes for RT-qPCR analysis in mouse testis development. *Mol Genet Genomics*. 2014; 289: 1157–1169. <https://doi.org/10.1007/s00438-014-0877-6> PMID: 24952483
 31. Spinazzi M, Casarin A, Pertegato V, Salviati L, Angelini C. Assessment of mitochondrial respiratory chain enzymatic activities on tissues and cultured cells. *Nat Protoc*. 2012; 7: 1235–1246. <https://doi.org/10.1038/nprot.2012.058> PMID: 22653162
 32. Seung H, Wolfe G, Rocca M. *Current Protocols in Toxicology*. 2003. pp. 16.7.1–16.7.6.
 33. Zogzas CE, Aschner M, Mukhopadhyay S. Structural Elements in the Transmembrane and Cytoplasmic Domains of the Metal Transporter SLC30A10 Are Required for Its Manganese Efflux Activity. *J Biol Chem*. 2016; 291: 15940–15957. <https://doi.org/10.1074/jbc.M116.726935> PMID: 27307044
 34. Nose Y, Wood LK, Kim B-E, Prohaska JR, Fry RS, Spears JW, et al. Ctr1 is an apical copper transporter in mammalian intestinal epithelial cells in vivo that is controlled at the level of protein stability. *J Biol Chem*. 2010; 285: 32385–32392. <https://doi.org/10.1074/jbc.M110.143826> PMID: 20699218
 35. Russell LD, Clegg ED, Ettl RA, Hikim APS. *Histological and histopathological evaluation of the testis*. 1st ed. Cache River Press; 1990. pp. 119–161.
 36. Wrobel KH, Bickel D, Kujat R. Immunohistochemical study of seminiferous epithelium in adult bovine testis using monoclonal antibodies against Ki-67 protein and proliferating cell nuclear antigen (PCNA). *Cell Tissue Res*. 1996; 283: 191–201. PMID: 8593648
 37. Goertz MJ, Wu Z, Gallardo TD, Hamra FK, Castrillon DH. Foxo1 is required in mouse spermatogonial stem cells for their maintenance and the initiation of spermatogenesis. *J Clin Invest*. 2011; 121: 3456–3466. <https://doi.org/10.1172/JCI57984> PMID: 21865646

38. Tarnawa ED, Baker MD, Aloisio GM, Carr BR, Castrillon DH. Gonadal Expression of Foxo1, but Not Foxo3, Is Conserved in Diverse Mammalian Species. *Biology of Reproduction*. 2013; 88: 489–11. <https://doi.org/10.1095/biolreprod.112.105791> PMID: 23486915
39. Richburg JH, Dwyer JL. The Sertoli cells as target for toxicants. In: McQueen CA, editor. *Comprehensive Toxicology*. 2nd ed. Elsevier Science; 2010. pp. 103–104.
40. Bertinato J, Iskandar M, L'Abbé MR. Copper deficiency induces the upregulation of the copper chaperone for Cu/Zn superoxide dismutase in weanling male rats. *J Nutr*. 2003; 133: 28–31. <https://doi.org/10.1093/jn/133.1.28> PMID: 12514262
41. Horn D, Barrientos A. Mitochondrial copper metabolism and delivery to cytochrome c oxidase. *IUBMB Life*. 2008; 60: 421–429. <https://doi.org/10.1002/iub.50> PMID: 18459161
42. Meinhardt A, Wilhelm B, Seitz J. Expression of mitochondrial marker proteins during spermatogenesis. *Hum Reprod Update*. 1999; 5: 108–119. PMID: 10336016
43. Hüttemann M, Jaradat S, Grossman LI. Cytochrome oxidase of mammals contains a testes-specific isoform of subunit VIb—the counterpart to testes-specific cytochrome c? *Mol Reprod Dev*. 2003; 66: 8–16. <https://doi.org/10.1002/mrd.10327> PMID: 12874793
44. Saunders PT, Millar MR, West AP, Sharpe RM. Mitochondrial cytochrome C oxidase II messenger ribonucleic acid is expressed in pachytene spermatocytes at high levels and in a stage-dependent manner during spermatogenesis in the rat. *Biology of Reproduction*. 1993; 48: 57–67. PMID: 8380346
45. Hess RA, Miller LA, Kirby JD, Margoliash E, Goldberg E. Immunoelectron microscopic localization of testicular and somatic cytochromes c in the seminiferous epithelium of the rat. *Biology of Reproduction*. 1993; 48: 1299–1308. PMID: 8391332
46. Narisawa S, Hecht NB, Goldberg E, Boatright KM, Reed JC, Millan JL. Testis-Specific Cytochrome c-Null Mice Produce Functional Sperm but Undergo Early Testicular Atrophy. *Mol Cell Biol*. 2002; 22: 5554–5562. <https://doi.org/10.1128/MCB.22.15.5554-5562.2002> PMID: 12101247
47. Kluin PM, Kramer MF, Rooij DG. Spermatogenesis in the immature mouse proceeds faster than in the adult. *International Journal of Andrology*. Blackwell Publishing Ltd; 1982; 5: 282–294. <https://doi.org/10.1111/j.1365-2605.1982.tb00257.x> PMID: 7118267
48. Kowal M, Lenartowicz M, Pecio A, Golas A, Błaszkiwicz T, Styrna J. Copper Metabolism Disorders Affect Testes Structure and Gamete Quality in Male Mice. *Systems Biology in Reproductive Medicine*. 2010; 56: 431–444. <https://doi.org/10.3109/19396361003734624> PMID: 20849226
49. Klomp AEM, Tops BBJ, Van Denberg IET, Berger R, Klomp LWJ. Biochemical characterization and subcellular localization of human copper transporter 1 (hCTR1). *Biochem J*. Portland Press Limited; 2002; 364: 497–505. <https://doi.org/10.1042/BJ20011803> PMID: 12023893
50. Blair BG, Larson CA, Adams PL, Abada PB, Pesce CE, Safaei R, et al. Copper Transporter 2 Regulates Endocytosis and Controls Tumor Growth and Sensitivity to Cisplatin In Vivo. *Molecular Pharmacology*. 2010; 79: 157–166. <https://doi.org/10.1124/mol.110.068411> PMID: 20930109
51. van den Berghe PVE, Folmer DE, Malingré HEM, van Beurden E, Klomp AEM, van de Sluis B, et al. Human copper transporter 2 is localized in late endosomes and lysosomes and facilitates cellular copper uptake. *Biochem J*. 2007; 407: 49–59. <https://doi.org/10.1042/BJ20070705> PMID: 17617060
52. Bertinato J, Swist E, Plouffe LJ, Brooks SPJ, L'Abbé MR. Ctr2 is partially localized to the plasma membrane and stimulates copper uptake in COS-7 cells. *Biochem J*. 2008; 409: 731–740. <https://doi.org/10.1042/BJ20071025> PMID: 17944601
53. Leichtmann-Bardoogo Y, Cohen LA, Weiss A, Marohn B, Schubert S, Meinhardt A, et al. Compartmentalization and regulation of iron metabolism proteins protect male germ cells from iron overload. *AJP: Endocrinology and Metabolism*. 2012; 302: E1519–E1530. <https://doi.org/10.1152/ajpendo.00007.2012> PMID: 22496346